Myosin Crossbridge, Contractile Unit, and the Mechanism of Contraction in Airway Smooth Muscle: A Mechanical Engineer's Perspective

Chun Y. Seow

Department of Pathology and
Laboratory Medicine,
Centre for Heart Lung Innovation,
University of British Columbia,
Vancouver, BC V6Z 1Y6, Canada
e-mail: chun.seow@hli.ubc.ca

Muscle contraction is caused by the action of myosin motors within the structural confines of contractile unit arrays. When the force generated by cyclic interactions between myosin crossbridges and actin filaments is greater than the average load shared by the crossbridges, sliding of the actin filaments occurs and the muscle shortens. The shortening velocity as a function of muscle load can be described mathematically by a hyperbola; this characteristic force–velocity relationship stems from stochastic interactions between the crossbridges and the actin filaments. Beyond the actomyosin interaction, there is not yet a unified theory explaining smooth muscle contraction, mainly because the structure of the contractile unit in smooth muscle (akin to the sarcomere in striated muscle) is still undefined. In this review, functional and structural data from airway smooth muscle are analyzed in an engineering approach of quantification and correlation to support a model of the contractile unit with characteristics revealed by mathematical analyses and behavior matched by experimental observation. [DOI: 10.1115/1.4042479]

Keywords: muscle contraction, length-force relationship, force-velocity relationship, myosin filament polymerization

Introduction

Muscle cells specialize in converting chemical energy to mechanical work. At the heart of the muscle "engine" are the myosin motors or crossbridges which are able to harness energy derived from adenosine triphosphate hydrolysis to drive their cyclic interactions with actin filaments leading to muscle contraction. Morphologically, the myosin molecules of striated and smooth muscle are indistinguishable. After they are activated, myosin crossbridges of smooth muscle interact with actin filaments in a qualitatively similar manner as their counterparts do in striated muscle [1,2]. The hyperbolic function which characterizes the force–velocity relationship in striated muscle [3] also describes the same relationship very well in smooth muscle [4–6]. This is taken as evidence suggesting that the molecular mechanism of the actomyosin interaction seen in striated muscle is also operative in smooth muscle.

A key difference between smooth and striated muscle appears to be in the myosin filament structure. Unlike the bipolar filaments found in striated muscle [7], myosin filaments in smooth muscle are likely side-polar [8–10]. This difference in the filament structure means that the contractile-unit structure in smooth muscle should be different from that of a striated muscle sarcomere, as envisioned by Craig and Megerman [8] and Hodgkinson et al. [11]; that is, a side-polar filament with crossbridges having the same polarity along the entire length of one side of the filament and opposite polarity on the other side and when interacting with actin filaments of matching polarities, pulling the actin filaments to slide in opposite directions (Fig. 1). The actin filaments (with a myosin filament sandwiched in between) are assumed to attach to dense bodies (equivalent to the Z-disks in striated muscle), thus

forming a functional contractile unit, at least in theory. In this review, functional and structural data from airway smooth muscle are analyzed with the help of mathematical models to test the validity of the side-polar contractile unit model. Mathematical models are also used to relate changes in force–velocity properties to changes in the kinetics of actomyosin crossbridge cycle and to explain why myosin filaments in smooth muscle, unlike those in striated muscle, do not have the same length.

Hill's Force–Velocity Hyperbola and Huxley's Crossbridge Kinetics

Hill, considered one of the founders of modern biophysics and a pioneer in systematically applying mathematical analysis in understanding biological phenomena, was the first to describe the
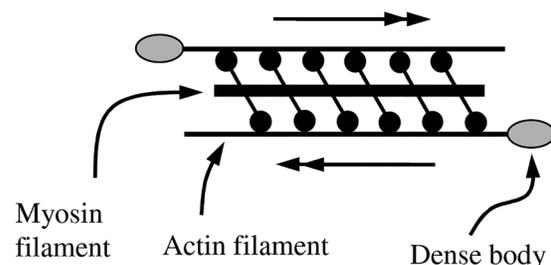
Fig. 1 A schematic depiction of a smooth muscle contractile unit consisting of a side-polar myosin filament with crossbridges on each side of the filament possessing opposite polarity, sandwiched by two actin filaments attached to dense bodies on one end. The double arrows indicate the direction of actin filament sliding relative to the myosin filament during active muscle shortening.

relationship between muscle force and velocity as a hyperbolic function [3]

$$(F + a)(V + b) = c \qquad (1)$$

where F and V are force and velocity and a, b, and c are constants. In the original measurements of heat production by muscle during contraction [3], it was believed that there was a link between constant a and shortening heat α, suggesting that the mechanical behavior of the muscle may be closely associated with energetic events occurring within the muscle cells. However, later measurements show that α is not a constant and the hyperbolic relationship between muscle force and shortening velocity is not a direct and simple reflection of energy utilization in the cell [12]. Therefore, the Hill equation for many decades had been used as an empirical equation for fitting force–velocity data from muscle experiments and was thought to have no connection whatsoever with the molecular mechanism of contraction [13], until recently. What changed our perception on the Hill equation and its physiological meaning is the recognition by Seow [14] that there is a direct linkage between the hyperbolic equation and Huxley's crossbridge models of muscle contraction [15,16].

To illustrate the linkage, we first rewrite the Hill equation in a normalized form and compare it to an equation derived from Huxley's two-state actomyosin kinetics [15]. Since the maximal shortening velocity (V_{max}) occurs when force (F) is zero, and at maximum isometric force (F_{max}), the velocity (V) is zero, from Eq. (1), we observe that $c = (F_{max} + a)b = (V_{max} + b)a$ or $a/F_{max} = b/V_{max}$. Hence, in the normalized form, a single constant can be used to represent a/F_{max} or b/V_{max}, i.e.,

$$K = a/F_{max} = b/V_{max} \qquad (2)$$

Therefore, in the normalized form ($F = F/F_{max}$, $V = V/V_{max}$), the Hill equation (Eq. (1)) becomes

$$F = \frac{K(1 - V)}{K + V} \qquad (3)$$

Next, we derive the relationship between force and velocity from Huxley's 1957 crossbridge model [15] (Fig. 2). In this model, the whole crossbridge population is assumed to reside in two states, the detached (D) and the attached (A) states. The fractions of the crossbridge populations sum up to one; i.e., $D + A = 1$.

A differential equation is used to calculate the rate of change of the crossbridge fraction in each state

$$dD/dt = g_{APP} \cdot A - f_{APP} \cdot D \qquad (4)$$

$$dA/dt = f_{APP} \cdot D - g_{APP} \cdot A \qquad (5)$$

where f_{APP} and g_{APP} are the apparent forward and reverse transition rates, respectively. We also know that

$$D + A = 1 \qquad (6)$$

In a steady-state, dD/dt and dA/dt are zero. The crossbridge fractions (D and A) in the steady-state can therefore be expressed
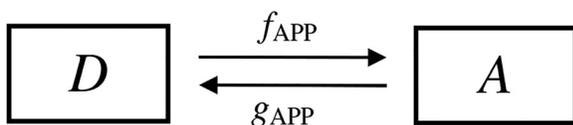
Fig. 2 A two-state model for the cycle of the actomyosin interaction. D, detached state; A, attached state. f_{APP} and g_{APP} are the apparent attachment and detachment rates.

as functions of the transition rates by simultaneously solving Eq. (6) and either Eq. (4) or Eq. (5). For example, from Eq. (4) (with $dD/dt = 0$), we have

$$A = D\left(\frac{f_{APP}}{g_{APP}}\right) \qquad (7)$$

Substituting A in Eq. (6) with Eq. (7)

$$D = \frac{g_{APP}}{g_{APP} + f_{APP}} \qquad (8)$$

Similarly

$$A = \frac{f_{APP}}{g_{APP} + f_{APP}} \qquad (9)$$

Designating p as force per attached crossbridge (or motor), the total force (F) produced by the muscle becomes

$$F = pA = p\left(\frac{f_{APP}}{g_{APP} + f_{APP}}\right) \qquad (10)$$

To transform Eq. (10) to a hyperbolic function of velocity, three prerequisites must be met (1) force per crossbridge declines linearly with shortening velocity, i.e., $p = 1 - V$, (2) the detachment rate is linearly proportional to the shortening velocity, i.e., $g_{APP} = kV$, where k is a proportionality constant, and (3) the attachment rate (f_{APP}) is independent of shortening velocity. The examination of data from Piazzesi et al. [17] revealed that all three prerequisites are met except at high forces or low velocities [14], where velocity data have also been shown to deviate from the hyperbolic curve [18–20].

With the three prerequisites in place, Eq. (10) becomes

$$F = (1 - V)\left(\frac{f_{APP}}{kV + f_{APP}}\right) \qquad (11)$$

and by defining

$$K = f_{APP}/k \qquad (12)$$

and from Eq. (11), we obtain $F = (1 - V)K/(V + K)$, which is exactly the same as the Hill equation (Eq. (3)).

The Hill equation is therefore a description of the Huxley crossbridge model under steady-state conditions when the muscle is not shortening against extreme high-loads. At intermediate range of loads where a muscle is operating at or near its maximal power and perhaps where the loads are most physiologically relevant, the Hill equation and the Huxley model are the same in terms of their mathematical expression and the associated insights into the molecular mechanisms. The Hill equation is therefore no longer just an empirical tool but contains mechanistic information of the crossbridge cycle. For example, because K is related to the curvature of a force–velocity curve [14], an increase in K will decrease the curvature and thus increase the relative power output of the muscle. Because $K = f_{APP}/k$ (Eq. (12)), we now know that an increase in muscle power can result from an increase in the apparent attachment rate (f_{APP}) and/or a decrease in k, or in other words, a decrease in the dependence of the apparent detachment rate (g_{APP}) on shortening velocity.

The Hill equation is related not only to the Huxley two-state model [15], but also to multi-state models [14]. Hill and Huxley were contemporaries and had a close personal and professional relationship. Undoubtedly many of their conversations were about theories of muscle contraction. Unfortunately, data on the molecular basis of force–velocity relations [17] were not available in their time for them to make the connection between their most important contributions to the understanding of muscle physiology.

Length–Force Relationship and the Time-Course of Isotonic Shortening

To accommodate the side-polar feature of the myosin filaments in smooth muscle [8], a contractile-unit structure different from that of striated muscle and similar to that shown in Figs. 1 and 3(a) has been proposed [11]. Although there is anecdotal evidence supporting such a model [21,22], structural and functional details of the model have yet to be substantiated. The distinct features in the length–force relationship of striated muscle (shown in gray in Fig. 4) stem directly from physical limitations associated with the unique sarcomeric structure of the muscle [23]; in other words, the sarcomeric structure determines the length–force relationship. The contractile-unit model for smooth muscle (Fig. 3(a)) predicts that the ascending limb of the length–force curve should be a straight line without a kink (Fig. 3b), unlike that of striated muscle (Fig. 4, gray lines) where a kink in the ascending portion of the curve is evident due to the encounter of the myosin filament with the Z-disk of the sarcomere during excessive shortening. Without a Z-disk in the smooth muscle contractile unit which contains dense bodies instead, such a kink is not expected in the length–force relationship of smooth muscle. Herrera et al. [22] tested the model (Fig. 3(a)) by measuring the lengths of airway smooth muscle at different isotonic loads while minimizing length adaptation during the measurement and confirmed that indeed, the ascending limb of the length–force curve in the muscle was a straight line (solid line and open circles, Fig. 4). The obvious lack of a kink in the ascending limb of the length–force curve indicates that the sarcomeric structure seen in striated muscle is unlikely to

Fig. 4 Length–force relationship of airway smooth muscle (solid line with open circles) compared with that of skeletal muscle (gray lines). Lengths are expressed as fractions of the muscle's in situ length designated as a reference length (L_{ref}); forces are expressed as fractions of the muscle's maximal isometric force (F_{max}). Modified from Seow (2016, *Introduction to Smooth Muscle Mechanics: Length-Force Relationship and Length Adaptation*, Friesen Press, Victoria, BC, pp. 109–131) with permission.

be present in smooth muscle; and furthermore, the data (Fig. 4) are consistent with the model shown in Fig. 3(a).

As suggested by the model (Fig. 3(a)), when smooth muscle shortens, its ability to generate force decreases linearly with respect to its length due to a linear decrease in the amount of overlap between the myosin and actin filaments. That is, the number of working crossbridges decreases as a muscle shortens. This means that the load shared by each crossbridge will increase as contraction proceeds even if the muscle is shortening against a constant load. The increasing load per crossbridge (due to the reduction in filament overlap and the resulting decrease in the working crossbridge number) will result in a continuous decrease in the overall shortening velocity of the muscle, if the model is correct. This theory can be presented as a mathematical model.

The length–force (L-F) relationship (Fig. 4, solid line) can be described by a linear function

$$F(L) = F_i + [(F_{max} - F_i)/(L_{ref} - L_i)](L - L_i)$$

where F_i is an arbitrarily chosen isotonic force (in the range of $0 < F_i < F_{max}$) and L_i is the maximally shortened length under the corresponding isotonic load. By expressing length and force values as fractions of L_{ref} and F_{max}, respectively

$$F(L) = F_i + \left(\frac{1 - F_i}{1 - L_i}\right)(L - L_i) \tag{13}$$

The shortening velocity as a function of both F and L can be obtained by modifying the Hill equation (Eq. (3)) and replacing F_{max} with $F(L)$

$$V = \frac{K(F(L) - F_i)}{K + F_i} \tag{14}$$

By setting $V = -(dL/dt)$ (where the negative sign indicates decreasing length) and combining Eqs. (13) and (14)

$$\frac{dL}{dt} = \frac{-mK(L - L_i)}{K + F_i} \tag{15}$$

where $((1 - F_i)/(1 - L_i)) = m$, i.e., the slope of the linear length–force curve (Fig. 4, solid line).

Fig. 3 A model of the contractile filament lattice illustrating the relationship between force generated by a contractile unit and the length of the overlap between myosin and actin filaments ($L_{overlap}$). An assumption associated with the model is that the force generated by a contractile unit is directly proportional to the overlap length. A: A change in $L_{overlap}$ due to shortening of a contractile unit from $L_{overlap1}$ to $L_{overlap2}$. B: The model predicts a linear relationship between force and $L_{overlap}$.

Fig. 5 (a) Mathematical simulation of the time course of an isotonic contraction in smooth muscle. Shortening starts at time zero from a reference length (L_{ref}) toward a final length (L_i) with a time constant ($-mK/[K + F_i]$) defined by Eq. (19). (b) Experimental data from an isotonic quick-release (circles) fitted with an exponential equation (Eq. (19)) after taking into account the viscoelastic recoil associated with the isotonic quick-release (solid line). Modified from Ref. [25] with permission.

Rearranging Eq. (15)

$$\int_1^L \frac{dL}{L - L_i} = \frac{-mK}{K + F_i} \int_0^t dt \tag{16}$$

Integrating Eq. (16) to obtain

$$\ln\left(\frac{L - L_i}{1 - L_i}\right) = \frac{-mK}{K + F_i} t \tag{17}$$

Or

$$\left(\frac{L - L_i}{1 - L_i}\right) = e^{\frac{-mK}{K + F_i} t} \tag{18}$$

Rearranging Eq. (18)

$$L = L_i + (1 - L_i) e^{\frac{-mK}{K + F_i} t} \tag{19}$$

Mathematical modeling therefore concludes that an exponential function should describe well the time course of isotonic shortening of smooth muscle, as illustrated in Fig. 5. Slowing of shortening velocity during an isotonic contraction in smooth muscle sometimes is interpreted as a reflection of the presence of an internal load [24]. With insights derived from mathematical modeling described above, it is apparent that continuous slowing of velocity during an isotonic contraction is a reflection of the decreasing overlap between myosin and actin filaments in the contractile units as illustrated in Fig. 3(a). Detailed analysis by Syyong et al. [25] concludes that the change in the contractile filament overlap is the dominant factor determining the time course of isotonic shortening, even though other factors such as internal loads may
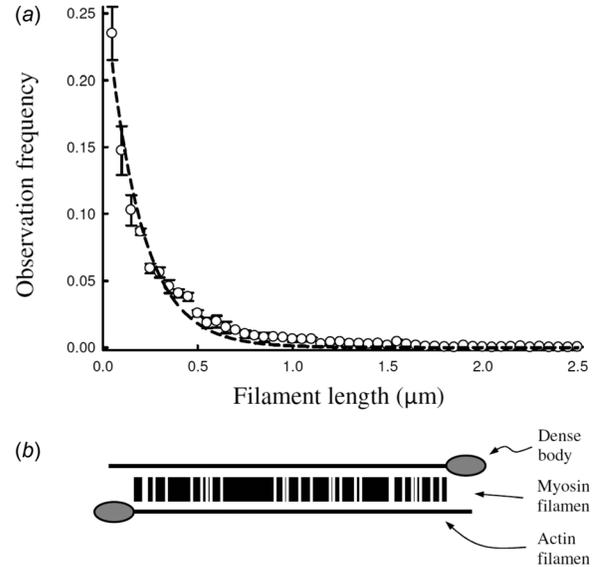
Fig. 6 (a) Length distribution of airway smooth muscle myosin filaments. The dashed line is a simple exponential fit to the data (open circles). Modified from Ref. [26] with permission. (b) Myosin filaments within an actin-filament lattice. The single continuous myosin filament shown in Fig. 3(a) is reproduced here as segments of filaments of different lengths lined up end-to-end to accommodate the observation of filament length distribution shown in panel (a).

be present. The exponential time course of isotonic shortening observed in smooth muscle can be taken as supporting evidence for the side-polar model of the contractile unit (Fig. 3(a)).

Myosin Filament Length and the Mechanism of Filament Formation

Myosin filament is an integral part of a contractile unit. So far, there is only one study that provided information on the frequency distribution of myosin filament lengths in smooth muscle [26]. Surprisingly, the distribution does not follow a Gaussian pattern but a pattern of exponential decay (Fig. 6). Although a mean length can be obtained from the distribution, more meaningful information can be obtained from the distribution itself. In fact, the exponential distribution suggests that myosin filaments in smooth muscle exist because of a dynamic equilibrium between two opposing processes, i.e., those of filament formation (polymerization of dimers by adding and subtracting the dimers at both ends of a filament) and fragmentation of existing filaments.

A mathematical model is developed to describe the dynamic process of linear aggregation and fragmentation. In the model, we consider a simple linear one-dimensional polymerization process where at each "time-step," bonds are formed between the dimers with probability p and are simultaneously broken with probability q. This dynamic process, when given enough time, will settle into a steady-state. In such a state, filament length distribution can be observed in a muscle cell fixed in a steady-state, such as the relaxed state or at the plateau of an isometric contraction.

Before reaching a steady-state (or equilibrium), the two competing processes, aggregation (formation of linear bonds between neighboring polymerization units) and fragmentation (breaking of the bonds) occur independently and randomly but with certain probabilities. For a total of N_{max} sites (i.e., maximal number of sites along a linear array of myosin dimers where bonds (n) can be made or broken between neighboring dimers), an equation describing the evolution of the mean number of n bonds is

$$\frac{dn}{dt} = (N_{max} - n)p - nq \tag{20}$$

The right-side first term describes the formation of bonds at $(N_{max} - n)$ possible sites, and the second term is the decay of existing bonds. For $q > 0$, this equation has a dynamic equilibrium or steady-state where $dn/dt = 0$, and $n = n_{eq}$, where n_{eq} represents a constant population of n at equilibrium. Under this condition, we obtain the mean probability r for the existence of an intact bond

$$r = \frac{n_{eq}}{N_{max}} = \frac{p}{p + q} \tag{21}$$

To obtain the distribution of filament length (i.e., the arrays of dimers linearly bonded together in this dynamic equilibrium), all probabilities are assumed to be independent and follow a binomial distribution, and we are simply considering a line of sites or bonds that are occupied with probability r. The probability P to observe a cluster of linearly connected x number of dimers is proportional to r^x, i.e.,

$$P(x) \propto r^x \tag{22}$$

This is analogous to the probability of obtaining x consecutive "heads" in coin tosses, which is $(1/2)^x$.

Because $r^x = e^{x \cdot \ln(r)}$, this equation describes a simple exponential decay

$$P(x) \propto e^{-x/\lambda} \tag{23}$$

where $\lambda = -1/\ln(r)$. λ is therefore the length constant in the exponential decay characterizing the myosin filament length distribution. Combine Eqs. (22) and (23), r can be expressed as a function of λ

$$r = e^{\frac{-1}{\lambda}} \tag{24}$$

Because

$$\lambda = \int_0^\infty e^{-x/\lambda} dx$$

the length distribution function can be normalized

$$P(x) = \frac{e^{-x/\lambda}}{\lambda} \tag{25}$$

Mathematical modeling therefore indicates that the probability or frequency of length distribution for myosin filaments in smooth muscle is a pure exponential decay function (Eq. (25)), and as it can be seen in Fig. 6, the model describes the data quite well.

The exponential distribution is quite different from the Gaussian distribution that has been observed in vitro when purified airway smooth muscle myosin molecules polymerize in a solution at a (unphysiological) low ionic strength of 80 mM [27]. At the relatively high physiological ionic strength of 200 mM, there is virtually no filament formation of smooth muscle myosin in vitro [28]. An intriguing question is why myosin filaments exist in smooth muscle cells. The answer could lie in the fact that myosin filament formation in smooth muscle occurs within the actin filament lattices, which are known to facilitate assembly of myosin filaments [29,30]. Many of the actin-filament-associated proteins such as caldesmon are also known to facilitate myosin filament assembly [31] perhaps due to their affinity to myosin molecules (see a review by Seow [32]). Recruitment of myosin molecules into the relatively restricted space of an actin filament lattice could be the catalytic step leading to myosin filament formation at physiological ionic strength. Within the lattice myosin molecules are not likely to form a long and unbroken filament as that shown in Fig. 3(a) but likely are in the form of filament segments lined up end-to-end as that shown in Fig. 6(b), with a length

distribution governed by an exponential decay function (Fig. 6(a)). Interestingly, if we only allow myosin polymerization and depolymerization to occur at the ends of a filament in the modeling, then a Gaussian distribution of the filament lengths appears [26]. The fact that exponential distribution is observed indicates that spontaneous fragmentation of a filament is not restricted to the two ends of the filament.

Mathematics as a Tool for Understanding Cell Biology

As illustrated by the previous examples, mathematical analyses could lead to deeper understanding of experimentally observed biological processes. A link between the Hill equation and the Huxley crossbridge model can be established only through mathematical analysis. With such a link, kinetics of the actomyosin interaction at a molecular level can be revealed by measuring force–velocity properties of a muscle at the tissue level. The hypothetical model of the smooth muscle contractile unit (Fig. 6(b)) now has an additional piece of supporting evidence because of mathematical modeling. The exponential distribution of myosin filament lengths in smooth muscle is not just a statement of experimental observation; with mathematical analysis, it allows us to speculate on the mechanism of myosin filament formation in a side-polar fashion and indirectly refutes the bipolar model (which is adopted by striated muscles) as the blue-print for myosin filaments of smooth muscle.

Funding Data

References

[1] Harris, D. E., and Warshaw, D. M., 1993, "Smooth and Skeletal Muscle Actin Are Mechanically Indistinguishable in the In Vitro Motility Assay," Circ. Res., **72**(1), pp. 219–224.

[2] Guilford, W. H., Dupuis, D. E., Kennedy, G., Wu, J., Patlak, J. B., and Warshaw, D. M., 1997, "Smooth Muscle and Skeletal Muscle Myosins Produce Similar Unitary Forces and Displacements in the Laser Trap," Biophys. J., **72**(3), pp. 1006–1021.

[3] Hill, A. V., 1938, "The Heat of Shortening and the Dynamic Constants of Muscle," Proc. R. Soc. London B Biol. Sci., **126**(843), pp. 136–195.

[4] Kamm, K. E., and Stull, J. T., 1985, "Myosin Phosphorylation, Force, and Maximal Shortening Velocity in Neurally Stimulated Tracheal Smooth Muscle," Am. J. Physiol., **249**(3), pp. C238–C247.

[5] Seow, C. Y., and Stephens, N. L., 1986, "Force-Velocity Curves for Smooth Muscle: Analysis of Internal Factors Reducing Velocity," Am. J. Physiol., **251**(3), pp. C362–C368.

[6] Warshaw, D. M., 1987, "Force: Velocity Relationship in Single Isolated Toad Stomach Smooth Muscle Cells," J. Gen. Physiol., **89**(5), pp. 771–789.

[7] Squire, J. M., 1975, "Muscle Filament Structure and Muscle Contraction," Annu. Rev. Biophys. Bioeng., **4**(00), pp. 137–163.

[8] Craig, R., and Megerman, J., 1977, "Assembly of Smooth Muscle Myosin Into Side-Polar Filaments," J. Cell Biol., **75**(3), pp. 990–996.

[9] Cooke, P. H., Fay, F. S., and Craig, R., 1989, "Myosin Filaments Isolated From Skinned Amphibian Smooth Muscle Cells Are Side-Polar," J. Muscle Res. Cell Motil., **10**(3), pp. 206–220.

[10] Xu, J. Q., Harder, B. A., Uman, P., and Craig, R., 1996, "Myosin Filament Structure in Vertebrate Smooth Muscle," J. Cell Biol., **134**(1), pp. 53–66.

[11] Hodgkinson, J. L., Newman, T. M., Marston, S. B., and Severs, N. J., 1995, "The Structure of the Contractile Apparatus in Ultrarapidly Frozen Smooth Muscle: Freeze-Fracture, Deep-Etch, and Freeze-Substitution Studies," J. Struct. Biol., **114**(2), pp. 93–104.

[12] Hill, A. V., 1964, "The Effect of Load on the Heat of Shortening of Muscle," Proc. R. Soc. London B Biol. Sci., **159**(975), pp. 297–318.

[13] Abbott, B. C., and Wilkie, D. R., 1953, "The Relation Between Velocity of Shortening and the Tension-Length Curve of Skeletal Muscle," J. Physiol., **120**(1–2), pp. 214–223.

[14] Seow, C. Y., 2013, "Hill's Equation of Muscle Performance and Its Hidden Insight on Molecular Mechanisms," J. Gen. Physiol., **142**(6), pp. 561–573.

[15] Huxley, A. F., 1957, "Muscle Structure and Theory of Contraction," Prog. Biophys. Biophys. Chem., **7**, pp. 255–318.

[16] Huxley, A. F., and Simmons, R. M., 1971, "Proposed Mechanism of Force Generation in Striated Muscle," Nature, **233**(5321), pp. 533–538.

[17] Piazzesi, G., Reconditi, M., Linari, M., Lucii, L., Bianco, P., Brunello, E., Decostre, V., Stewart, A., Gore, D. B., Irving, T. C., Irving, M., and Lombardi, V., 2007, "Skeletal Muscle Performance Determined by Modulation of Number of Myosin Motors Rather Than Motor Force or Stroke Size," Cell, **131**(4), pp. 784–795.

[18] Edman, K. A., 1988, "Double-Hyperbolic Force-Velocity Relation in Frog Muscle Fibres," J. Physiol., **404**, pp. 301–321.

[19] Wang, J., Jiang, H., and Stephens, N. L., 1994, "A Modified Force-Velocity Equation for Smooth Muscle Contraction," J. Appl. Physiol., **76**(1), pp. 253–258.

[20] Devrome, A. N., and MacIntosh, B. R., 2007, "The Biphasic Force-Velocity Relationship in Whole Rat Skeletal Muscle in Situ," J. Appl. Physiol., **102**(6), pp. 2294–2300.

[21] Bond, M., and Somlyo, A. V., 1982, "Dense Bodies and Actin Polarity in Vertebrate Smooth Muscle," J. Cell Biol., **95**(2 Pt. 1), pp. 403–413.

[22] Herrera, A. M., McParland, B. E., Bienkowska, A., Tait, R., Paré, P. D., and Seow, C. Y., 2005, "Sarcomeres' of Smooth Muscle: Functional Characteristics and Ultrastructural Evidence," J. Cell Sci., **118**(11), pp. 2381–2392.

[23] Gordon, A. M., Huxley, A. F., and Julian, F. J., 1966, "The Variation in Isometric Tension With Sarcomere Length in Vertebrate Muscle Fibres," J. Physiol., **184**(1), pp. 170–192.

[24] Harris, D. E., and Warshaw, D. M., 1990, "Slowing of Velocity During Isotonic Shortening in Single Isolated Smooth Muscle Cells. Evidence for an Internal Load," J. Gen. Physiol., **96**(3), pp. 581–601.

[25] Syyong, H. T., Raqeeb, A., Paré, P. D., and Seow, C. Y., 2011, "Time Course of Isotonic Shortening and the Underlying Contraction Mechanism in Airway Smooth Muscle," J. Appl. Physiol., **111**(3), pp. 642–656.

[26] Liu, J. C., Rottler, J., Wang, L., Zhang, J., Pascoe, C. D., Lan, B., Norris, B. A., Herrera, A. M., Paré, P. D., and Seow, C. Y., 2013, "Myosin Filaments in Smooth Muscle Cells Do Not Have a Constant Length," J. Physiol., **591**(23), pp. 5867–5878.

[27] Ip, K., Sobieszek, A., Solomon, D., Jiao, Y., Paré, P. D., and Seow, C. Y., 2007, "Physical Integrity of Smooth Muscle Myosin Filaments Is Enhanced by Phosphorylation of the Regulatory Myosin Light Chain," Cell. Physiol. Biochem., **20**(5), pp. 649–658.

[28] Rovner, A. S., Fagnant, P. M., Lowey, S., and Trybus, K. M., 2002, "The Carboxyl-Terminal Isoforms of Smooth Muscle Myosin Heavy Chain Determine Thick Filament Assembly Properties," J. Cell Biol., **156**(1), pp. 113–123.

[29] Mahajan, R. K., Vaughan, K. T., Johns, J. A., and Pardee, J. D., 1989, "Actin Filaments Mediate Dictyostelium Myosin Assembly In Vitro," Proc. Natl. Acad. Sci. U. S. A., **86**(16), pp. 6161–6165.

[30] Applegate, D., and Pardee, J. D., 1992, "Actin-Facilitated Assembly of Smooth Muscle Myosin Induces Formation of Actomyosin Fibrils," J. Cell Biol., **117**(6), pp. 1223–1230.

[31] Katayama, E., Scott-Woo, G., and Ikebe, M., 1995, "Effect of Caldesmon on the Assembly of Smooth Muscle Myosin," J. Biol. Chem., **270**(8), pp. 3919–3925.

[32] Seow, C. Y., 2005, "Myosin Filament Assembly in an Ever-Changing Myofilament Lattice of Smooth Muscle," Am. J. Physiol. Cell Physiol., **289**(6), pp. C1363–C1368.